

Supplementary Data

The cytosolic DNA sensor AIM2 promotes KRAS-driven lung cancer independent of inflammasomes

Mohammad Alanazi, Teresa Weng, Louise McLeod, Linden J. Gearing, Julian A. Smith, Beena Kumar, Mohamed I. Saad, Brendan J. Jenkins

Supplementary figure 1: Gene expression analysis of cytosolic DNA sensors, and AIM2 and cleaved Caspase-1 immunohistochemical staining, in human lung biopsies from lung adenocarcinoma (LAC) patients and non-cancer controls.

Supplementary figure 2: Genetic ablation of AIM2 in *Kras*^{G12D} mice suppresses the LAC phenotype.

Supplementary figure 3: Suppressed cellular proliferation in the lung parenchyma of *Kras*^{G12D} mice upon genetic ablation of AIM2.

Supplementary figure 4: Deficiency of AIM2 does not affect expression of inflammasome-associated components, nor activation of NF- κ B and Akt signaling cascades, in the lungs of *Kras*^{G12D} mice.

Supplementary figure 5: Deficiency of AIM2 impairs activation of p38 MAPK signaling, independent of IL-1 β production, in the lungs of mice administered with NNK.

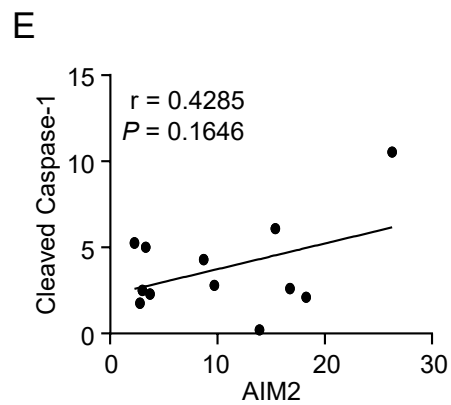
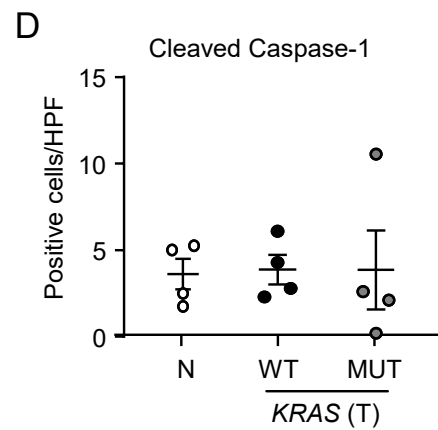
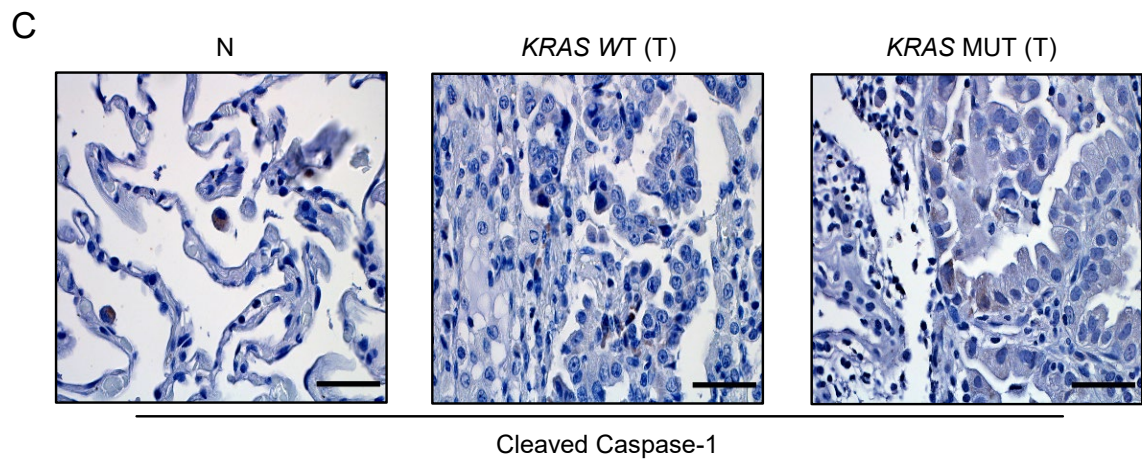
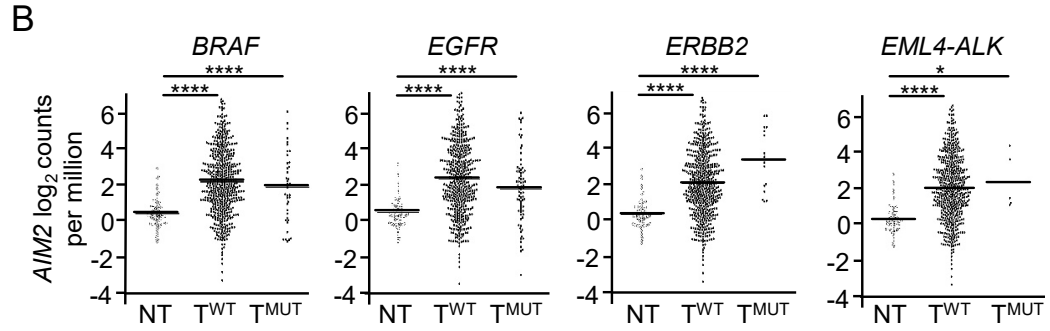
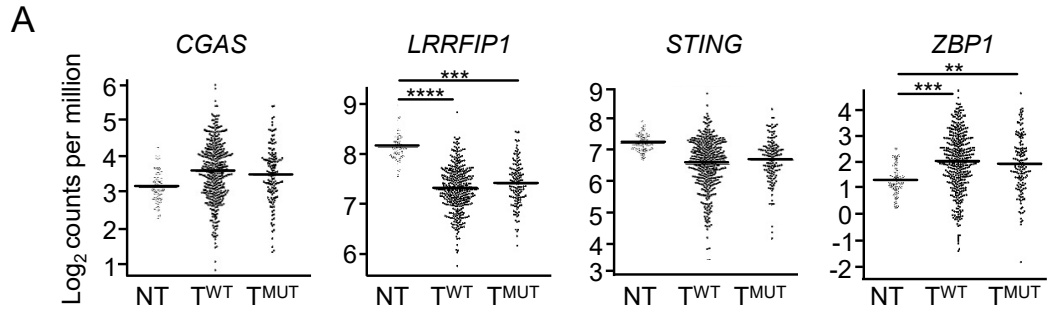
Supplementary figure 6: Genetic ablation of ASC in the lungs of *Kras*^{G12D} mice does not suppress the LAC phenotype, nor inflammasome-associated maturation of Caspase-1 and IL-1 β .

Supplementary table 1: Clinicopathological characteristics of patients for gene expression, immunohistochemistry and/or immunofluorescence assays.

Supplementary figure 1:

Gene expression analysis of cytosolic DNA sensors, and AIM2 and cleaved Caspase-1 immunohistochemical staining, in human lung biopsies from lung adenocarcinoma (LAC) patients and non-cancer controls.

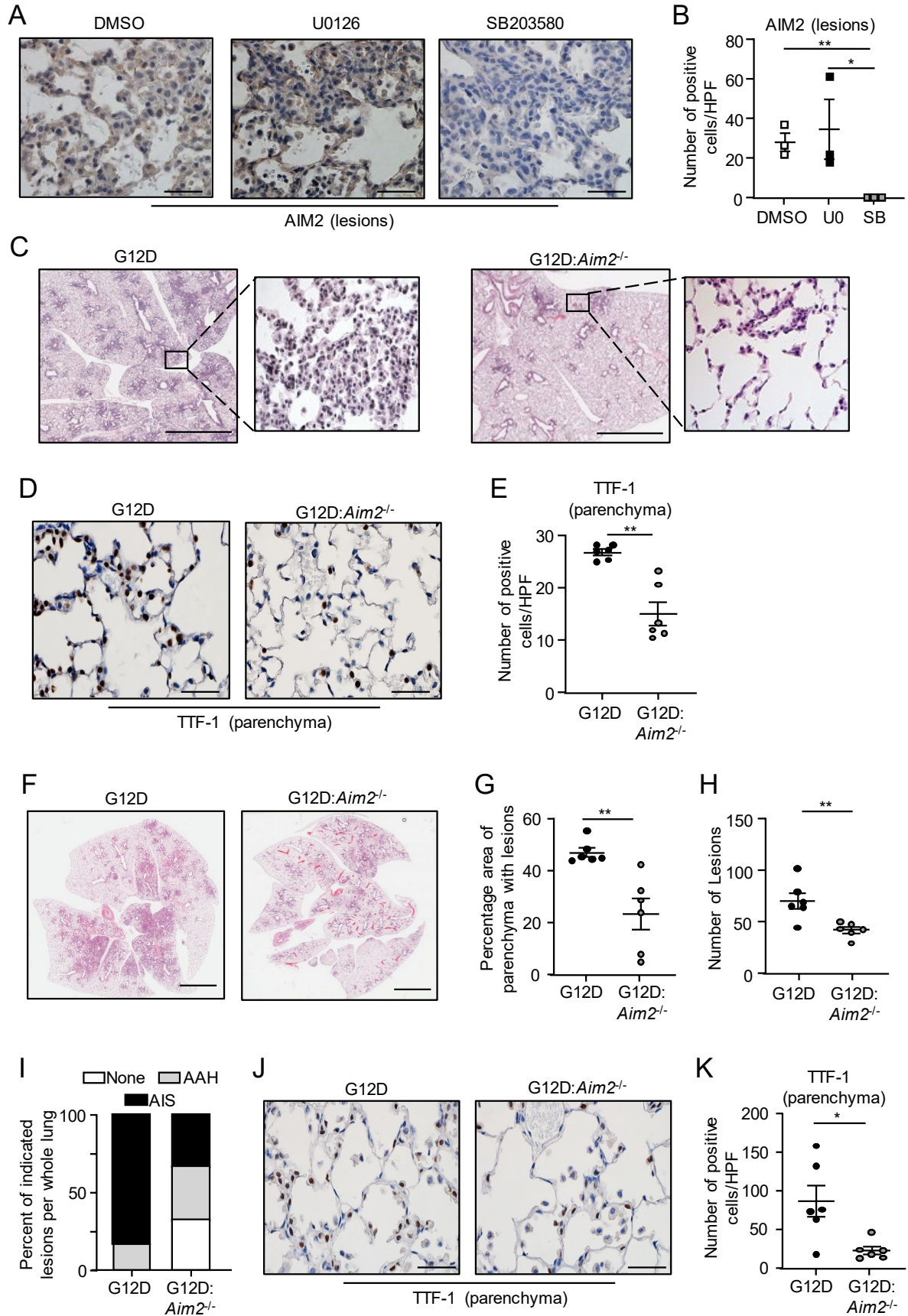
A, Gene expression analysis of representative cytosolic DNA sensors in *KRAS* mutant (MUT) tumour (T; n = 138) and *KRAS* wild-type (WT) tumour (n = 375) versus non-tumour (NT; n = 59) tissues from TCGA LAC patients. False-discovery rate adjusted *P* values: ***P*<0.01, ****P*<0.001, *****P*<0.001. **B**, Gene expression analysis of *AIM2* in the indicated molecular subtypes classified by mutant status of tumour tissues versus wild-type tumour and non-tumour (n = 59) tissues from TCGA LAC patients. *BRAF*, mutant (n = 39) and wild-type (n = 474); *EGFR*, mutant (n = 73) and wild-type (n = 440); *ERBB2*, mutant (n = 16) and wild-type (n = 497); *EML4-ALK*, mutant (n = 5) and wild-type (n = 508). False-discovery rate adjusted *P* values: **P*<0.05, *****P*<0.001. **C**, Representative images of cleaved (p20) Caspase-1-stained lung sections from normal (N) non-cancer control tissues, as well as tumour (T) tissues from LAC patients stratified into either *KRAS* wild-type (WT) or *KRAS* mutant (MUT). Scale bars = 100µm. **D**, Quantification of cleaved Caspase-1-positive cells per high-power field (HPF) in the indicated groups of human lung biopsies (n = 4 per group). **E**, Linear regression analyses of cleaved Caspase-1 and *AIM2* immunohistochemical staining in serial lung human sections from the indicated groups in panel B. *r*, Pearson correlation coefficient.



Supplementary figure 2:

Genetic ablation of AIM2 in *Kras*^{G12D} mice suppresses the LAC phenotype.

A, Representative images of AIM2-stained lung sections from *Kras*^{G12D} mice (6 weeks post Ad-Cre inhalation) treated with a single dose of either SB203580 p38 MAPK inhibitor, U0126 ERK1/2 inhibitor or dimethyl sulfoxide (DMSO) vehicle (control). Scale bars = 100µm. **B**, Quantification of AIM2 staining in tumour lesions of the indicated mouse treatment groups in panel A (n = 3/genotype). **P*<0.05, ***P*<0.01. **C**, Representative low power images (left) of H&E-stained lung sections from *Kras*^{G12D} and *Kras*^{G12D}:*Aim2*^{-/-} mice at 6 weeks post Ad-Cre inhalation. Scale bars (left images) = 3mm. Also shown are magnified images (right) of the depicted areas (open squares) in the corresponding low power images. **D**, Representative images of unaffected (i.e. histologically normal) areas of parenchyma in TTF-1-stained lung sections from *Kras*^{G12D} and *Kras*^{G12D}:*Aim2*^{-/-} mice at 6 weeks post Ad-Cre inhalation. Scale bars = 100µm. **E**, Quantification of TTF-1-positive cells/high power field (HPF) in lungs of the indicated genotypes (n = 6/genotype). ***P*<0.01, Student's *t*-test. **F**, Representative images of H&E-stained lung sections from *Kras*^{G12D} and *Kras*^{G12D}:*Aim2*^{-/-} mice at 12 weeks post Ad-Cre inhalation. Scale bars (left images) = 3mm. **G-I**, Quantification of (G) lung parenchyma area occupied by tumour lesions, (H) tumour incidence, and (I) lesion histological classification, per whole mouse lung in the indicated genotypes at 12 weeks post Ad-Cre inhalation (n = 6/genotype). ***P*<0.01, Student's *t*-test. AAH, atypical adenomatous hyperplasia; AIS, adenocarcinoma *in situ*. **J**, Representative images of unaffected (i.e. histologically normal) areas of parenchyma in TTF-1-stained lung sections from *Kras*^{G12D} and *Kras*^{G12D}:*Aim2*^{-/-} mice at 12 weeks post Ad-Cre inhalation. Scale bars = 100µm. **K**, Quantification of TTF-1-positive cells/HPF in lungs of the indicated genotypes at 12 weeks post Ad-Cre inhalation (n = 6/genotype). **P*<0.05, Student's *t*-test.



Supplementary figure 3:

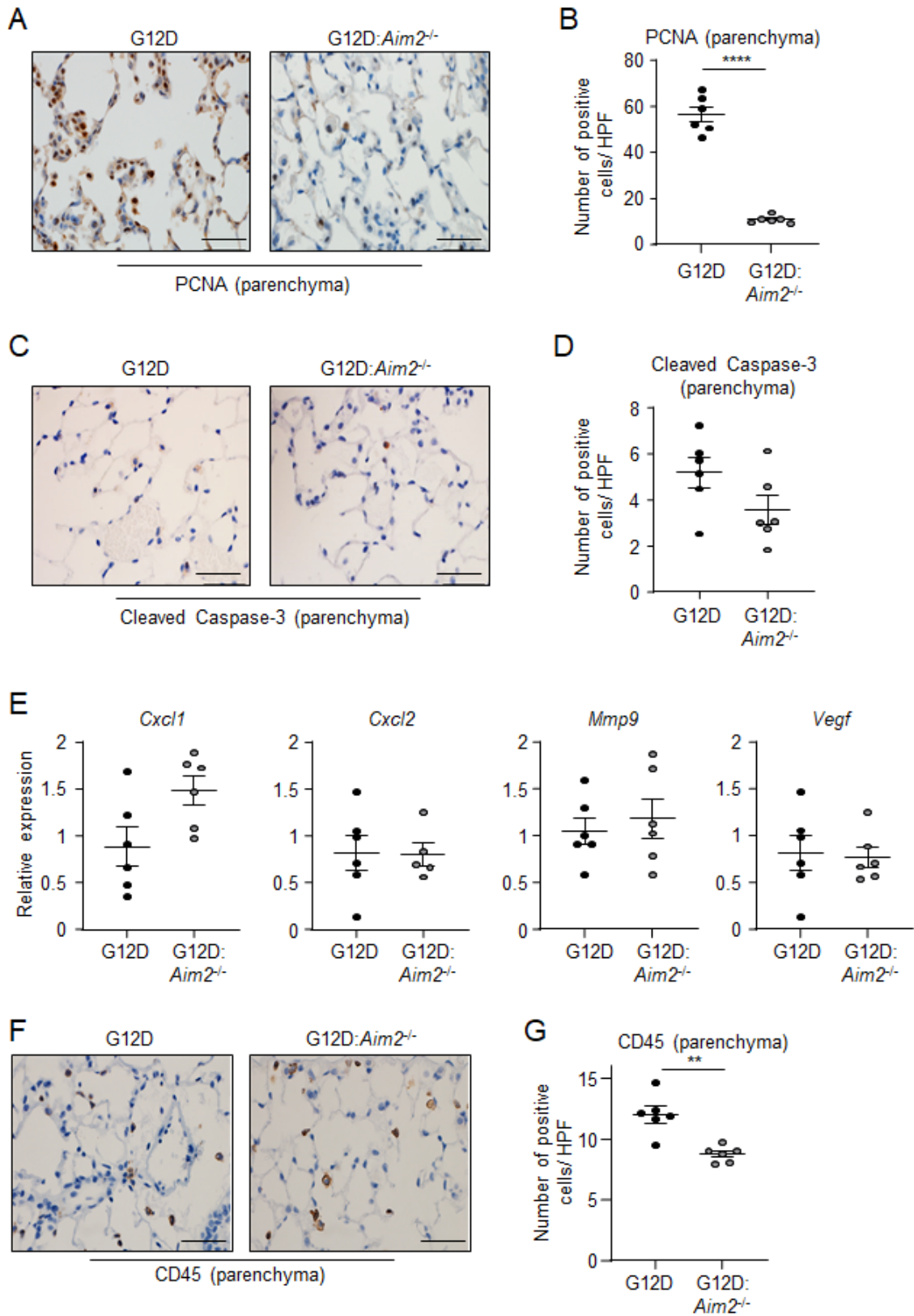
Suppressed cellular proliferation in the lung parenchyma of *Kras*^{G12D} mice upon genetic ablation of AIM2.

A and **C**, Representative images of unaffected (i.e. histologically normal) areas of parenchyma in (A) PCNA-stained and (C) cleaved Caspase-3-stained lung sections from *Kras*^{G12D} and *Kras*^{G12D}:*Aim2*^{-/-} mice at 6 weeks post Ad-Cre inhalation. Scale bars = 100µm.

B and **D**, Quantification of (B) PCNA-positive and (D) cleaved Caspase-3-positive cells/high power field (HPF) in lungs of the indicated genotypes (n = 6/genotype). *****P*<0.0001, Student's *t*-test.

E, qPCR analyses of angiogenesis genes (relative to the housekeeping gene *Rn18s*) in lung tissues of the indicated genotypes at 6 weeks post Ad-Cre inhalation (n = 6/genotype).

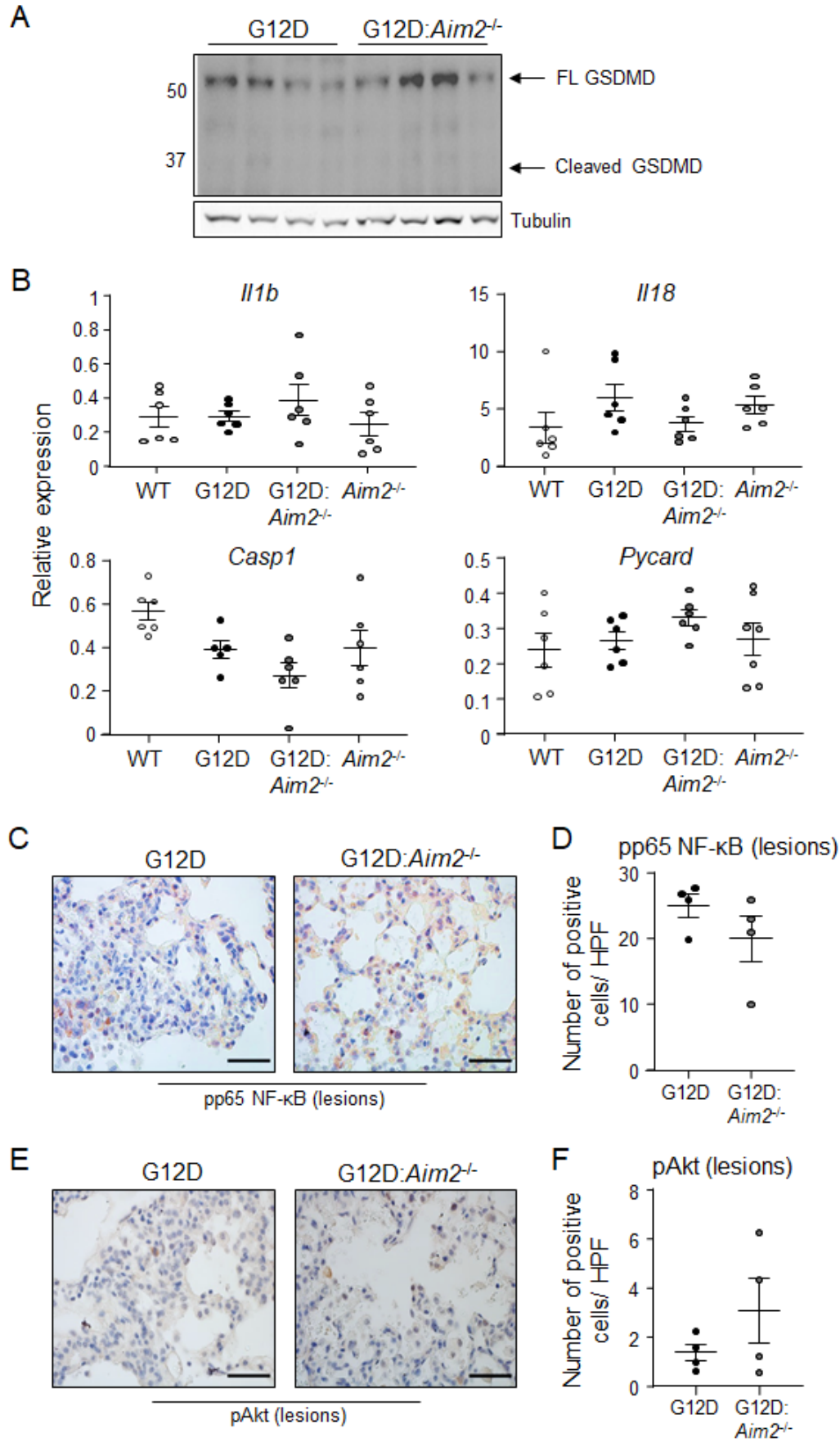
F and **G**, Shown are (F) representative images and (G) graphs depicting quantification of unaffected (i.e. histologically normal) areas of lung parenchyma sections from *Kras*^{G12D} and *Kras*^{G12D}:*Aim2*^{-/-} mice at 6 weeks post Ad-Cre inhalation stained with CD45 (n = 6/genotype). Scale bars = 100µm. ***P*<0.01, Student's *t*-test.



Supplementary figure 4:

Deficiency of AIM2 does not affect expression of inflammasome-associated components, nor activation of NF- κ B and Akt signaling cascades, in the lungs of *Kras*^{G12D} mice.

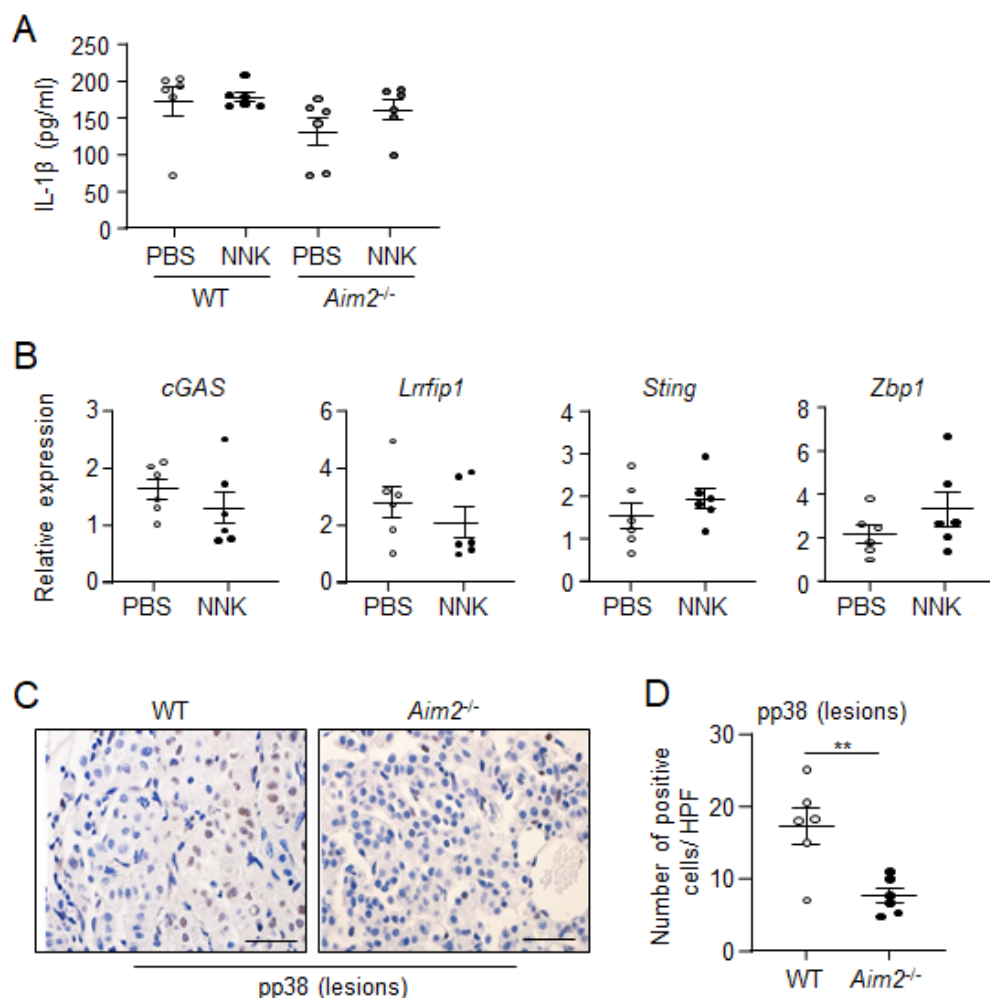
A, Immunoblotting with an antibody detecting full-length (FL) and cleaved (p31) forms of Gasdermin D (GSDMD) in whole lung lysates of *Kras*^{G12D} and *Kras*^{G12D}:*Aim2*^{-/-} mice at 6 weeks post Ad-Cre inhalation. An antibody against Tubulin is used as a loading control. Each lane represents tissue from an individual mouse. **B**, qPCR analyses of the indicated genes (relative to the housekeeping gene *Rn18s*) in lung tissues of *Kras*^{WT}, *Kras*^{G12D}, *Kras*^{G12D}:*Aim2*^{-/-} and *Aim2*^{-/-} mice at 6 weeks post Ad-Cre (*Kras*^{G12D}, *Kras*^{G12D}:*Aim2*^{-/-}) or PBS vehicle (*Kras*^{WT}, *Aim2*^{-/-}) inhalation. (n = 6/genotype). **C** and **E**, Representative images of (C) phosphorylated (p) p65 NF- κ B, and (E) pAkt immunostaining of lung sections containing lesions from *Kras*^{G12D} and *Kras*^{G12D}:*Aim2*^{-/-} mice at 6 weeks post Ad-Cre inhalation. Scale bars = 100 μ m. **D** and **F**, Quantification of (D) pp65 NF- κ B and (F) pAkt positively stained cells/high power field (HPF) in lung lesions of the indicated mice (n = 4/genotype).



Supplementary figure 5:

Deficiency of AIM2 impairs activation of p38 MAPK signaling, independent of IL-1 β production, in the lungs of mice administered with NNK.

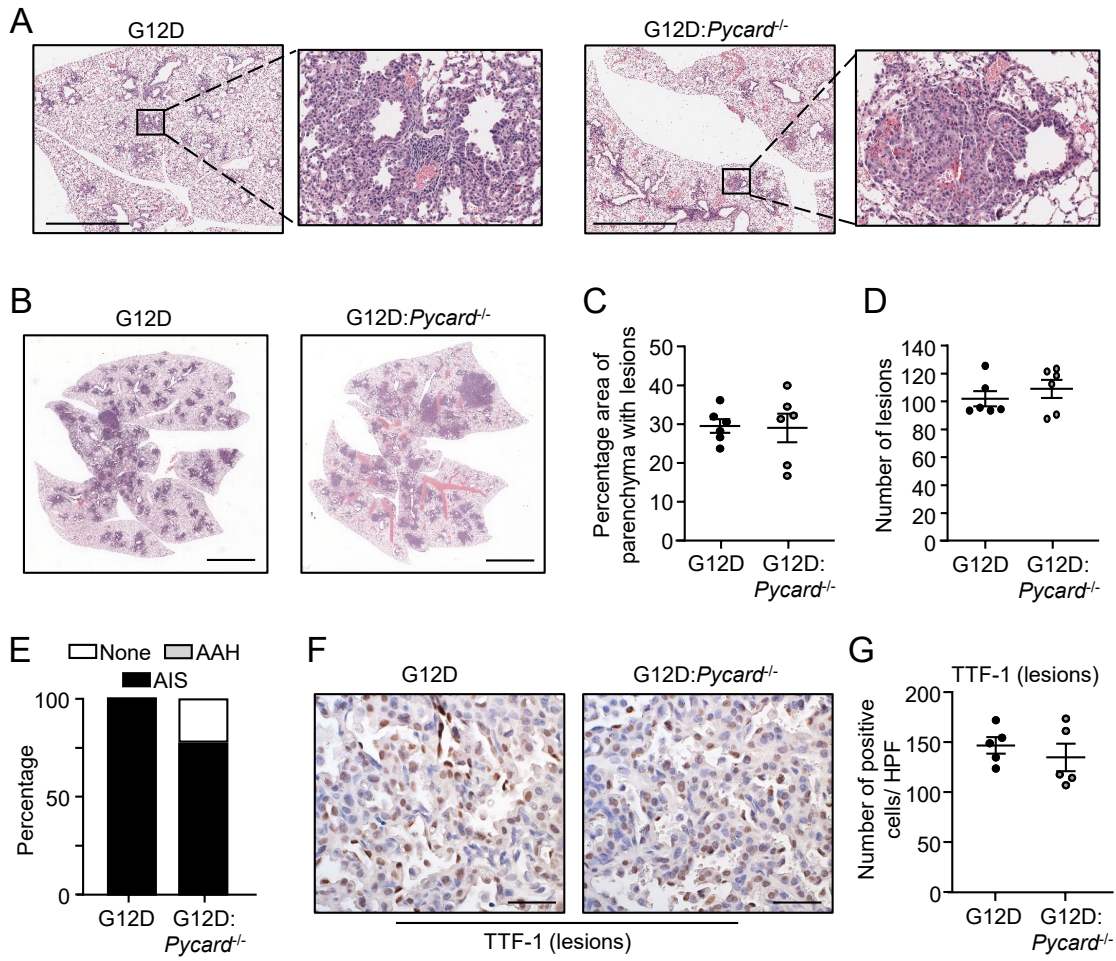
A, ELISA for total IL-1 β protein levels in the serum of the indicated mice at 20 weeks post NNK or PBS administration (n = 6/genotype). **B**, qPCR expression analyses of the indicated cytosolic DNA sensor genes (relative to the housekeeping gene *Rn18s*) in lungs from WT pseudo-A/J mice at 20 weeks post NNK or PBS administration (n = 6/genotype). * $P < 0.05$, Student's *t*-test. **C**, Representative images of phosphorylated (p) p38 MAPK immunostaining of lung sections containing lesions from WT and *Aim2*^{-/-} pseudo-A/J mice at 20 weeks post NNK administration. Scale bars = 100 μ m. **D**, Quantification of pp38 MAPK positively stained cells/high power field (HPF) in lung lesions of the indicated mice from panel (C) (n = 6/genotype). ** $P < 0.01$, Student's *t*-test.



Supplementary figure 6:

Genetic ablation of ASC in the lungs of *Kras*^{G12D} mice does not suppress the LAC phenotype, nor inflammasome-associated maturation of Caspase-1 and IL-1 β .

A, Representative low power images (left) of H&E-stained lung sections from *Kras*^{G12D} and *Kras*^{G12D}:*Pycard*^{-/-} mice at 6 weeks post Ad-Cre inhalation. Scale bars (left images) = 1mm. Also shown are magnified images (right) of the depicted areas (open squares) in the corresponding low power images. **B**, Representative images of H&E-stained lung sections from *Kras*^{G12D} and *Kras*^{G12D}:*Pycard*^{-/-} mice at 12 weeks post Ad-Cre inhalation. Scale bars = 3mm. **C-E**, Quantification of (C) lung parenchyma area occupied by tumour lesions, (D) tumour incidence, and (E) lesion histological classification, per whole mouse lung in the indicated genotypes at 12 weeks post Ad-Cre inhalation (n = 6/genotype). AAH, atypical adenomatous hyperplasia; AIS, adenocarcinoma *in situ*. **F**, Representative images of lung sections containing lesions from *Kras*^{G12D} and *Kras*^{G12D}:*Pycard*^{-/-} mice at 12 weeks post Ad-Cre inhalation. Scale bars = 100 μ m. **G**, Quantification of TTF-1-positive cells/HPF in lung lesions of the indicated genotypes at 12 weeks post Ad-Cre inhalation (n = 5/genotype).



Supplementary table 1:

Clinicopathological characteristics of patients for gene expression, immunohistochemistry and/or immunofluorescence assays¹.

	LAC	Non-LAC
Mean age		
Years (range)	66.6 (47-78)	58.3 (47-71)
Sex [number (%)]		
Male	12 (43)	6 (60)
Female	16 (57)	4 (40)
KRAS status [number (%)]		
Wild-type	14 (50)	NA
Mutant	14 (50)	NA
Tumour stage² [number (%)]		
I	12 (43)	NA
II	8 (28.5)	NA
Unknown	8 (28.5)	NA

¹Lung tissues were acquired by surgical resection from LAC patients and control LAC-free individuals at Monash Medical Centre, Clayton, Victoria, Australia

²American Joint Committee on Cancer staging for non-small cell lung cancer based on tumour (T)/node (N)/metastasis (M) classification; Stage I (IA/IB), Stage II (IIA/IIB), Stage III (IIIA/IIIB), Stage IV.

NA, not applicable. LAC, lung adenocarcinoma.